ACU Optimization of pcLEDs by Combining the Pulsed Spray and Feedback Method

Jia-Sheng Li, Yong-Hui Chen, Zong-Tao Li, Shu-Dong Yu, Yong Tang, Xin-Rui Ding, and Wei Yuan

***Abstract*—In this paper, the pulse-sprayed (PS) phosphor coating technique and feedback method were combined to optimize the angular color uniformity of remote phosphor-converted light-emitting diodes (pcLEDs). The geometry of the phosphor-converted element (PCE) was controlled by the PS technique and the curvature of the phosphor bearing surface. Meanwhile, the yellow and blue light irradiance distributions are as the feedback function to optimize the mass distribution of the PS PCE during the feedback iteration process. With the method proposed herein, the correlative color temperature of the optimized remote pcLED ranges from 5192 to 5263 K with a maximum deviation of only 71 K.**

***Index Terms*— angular color uniformity, feedback, Light-emitting diodes, pulsed spray, remote phosphor.**

I. Introduction

LIGHT-EMITTING diodes (LEDs) are one of the most promising solid lighting sources because of their many advantages such as low environmental impact and long life. Generally, blue chips are combined with phosphor-converted elements (PCEs) to obtain white LEDs, which are also called phosphor-converted LEDs (pcLEDs) [1]. At the present, to satisfy the increasing demands on pcLED optical performance, the quality of their emitted light requires significant improvement, especially in terms of angular color uniformity (ACU) [2]–[7]. Generally, the conformal phosphor structure helps to improve the ACU as it strongly scatters the blue light emitted from the LED chip [8]–[11]. However, this structure makes it difficult to achieve a high light efficiency (LE) due to the strong absorption of the backscattered light. Compared with the conformal phosphor structure, the remote phosphor structure can commonly achieve a higher LE because the backscattered light is less possible to be absorbed by chips [12], [13]. In order to fully utilize the high LE of remote phosphor structures while simultaneously achieving excellent ACU performance, it has been common to optimize their PCE structure, especially in terms of geometry [14]–[19]. However, the optimized PCEs in most of studies were achieved by the trial-and-error method, which it is difficult to ensure the ideal ACU. Feedback method, as one of the most efficient optimization methods, has already been used to obtain the specific correlated color temperature (CCT) of pcLEDs with multi-phosphor configurations [20]. However, to the best of our knowledge, it has not yet been used for ACU optimization because the CCT distribution is more difficult to be controlled.

From a practical point of view, it's important to take the phosphor coating approaches into consideration when optimizing the PCE. The pulse-sprayed (PS) technique, as an environmentally friendly and cost effective phosphor coating approach, has been widely studied in literatures [9], [21]–[23] and applied in LED products [24]. Its primary characteristic is that the phosphor mass per projection area along the spraying direction keeps constant, which was also studied in our previous work [25]. It can be expected that the PS PCE thickness has certain relationships to the curvature of the phosphor bearing surface.

In this study, we first present an investigation on the effect of the curvature of the phosphor bearing surface on the PCE geometry in the PS phosphor coating process, which is important for us to predict the geometry of the PS PCE being sprayed on the freeform phosphor bearing surface. Then we propose a pulsed spray and feedback (PSFB) combined method focused on improving the ACU of remote pcLEDs. The PCE geometry is controlled by the surface of the isolated layer (IL), that it's the phosphor bearing surface. Meanwhile, the mass distribution of the PS PCE is optimized by the feedback iteration process using the yellow/blue light irradiance distributions as feedback function. Finally the optimized results are given and discussed in detail.

II. Experiments

As the freeform phosphor bearing surface can be treated as being consisted with many flat surfaces, the stepped frustum with three different angles was used to investigate the effect of the curvature of the phosphor bearing surface on the PCE geometry. The fabrication of PCE was performed by the PS phosphor coating technique [25]. Firstly, the phosphor slurry was prepared by mixing the YAG: Ce phosphor, silicone and diluent, their overall ratios are 39.5%, 26.3% and 34.2%, respectively. To prevent the phosphor from settling before it was sprayed out, the phosphor slurry was disturbed mechanically. And the feed velocity of the nozzle along the x, y direction, the air pressure and the spraying frequency, were controlled to optimize the coating quality. Then, the phosphor slurry was sprayed onto the phosphor

Manuscript received November 17, 2015; revised January 8, 2016; accepted July 3, 2016. Date of publication July 7, 2016; date of current version September 13, 2016. This work was supported in part by the National Natural Science Foundation of China under Grants U1401249, 51375177, and 51405161, and in part by the Postdoctoral Science Foundation of China under Grant 2015T80904. *(Corresponding author: Zong-Tao Li.)*

J.–S. Li, Y.-H. Chen, S.-D. Yu, Y. Tang, and W. Yuan are with the Key Laboratory of Surface Functional Structure Manufacturing of Guangdong High Education Institutes, South China University of Technology, Guangzhou 510641, China (e-mail: qwd886me@qq.com; cheffy@yeah.net; yu.shudong@mail.scut.edu.cn; ytang@scut.edu.cn; mewyuan@scut.edu.cn).

Z.-T. Li is with the Key Laboratory of Surface Functional Structure Manufacturing of Guangdong High Education Institutes, South China University of Technology, Guangzhou 510641, China and also with the Foshan Nationstar Optoelectronics Company Ltd., Foshan 528000, China (e-mail: meztli@scut.edu.cn).

X.-R. Ding is with the Department of Mechanical Engineering, University of California at Berkeley, Berkeley, CA 94720-5800 USA (e-mail: ding.xinrui@mail.scut.edu.cn).

Color versions of one or more of the figures are available online at http://ieeexplore.ieee.org.

Digital Object Identifier 10.1109/JDT.2016.2588419

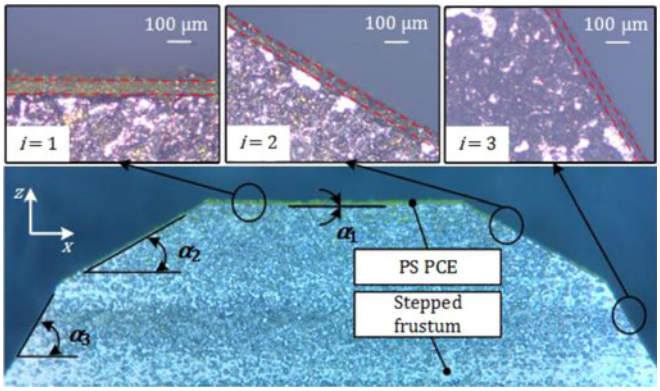

Fig. 1. The cross-section of the PS PCE coating on the phosphor bearing surface of the stepped frustum.

TABLE I
VALUES OF PARAMETERS α_i, t_i AND h_i

	$\alpha_1 = 0°$		$\alpha_2 = 30°$		$\alpha_3 = 60°$	
No.	t_1 (μm)	h_1 (μm)	t_2 (μm)	h_2 (μm)	t_3 (μm)	h_3 (μm)
1	56.41	56.41	48.25	55.71	32.00	64.00
2	61.53	61.53	50.02	57.76	28.01	56.02
3	59.24	59.24	52.40	60.51	28.04	56.08
4	59.61	59.61	53.15	61.37	28.68	57.36
5	60.87	60.87	52.48	60.60	30.26	60.52
6	60.24	60.24	50.02	57.76	32.60	65.20
Average	59.65	59.65	51.05	58.95	29.93	59.86

bearing surface through the air atomizing nozzle and was cured at a temperature of 150 °C for 5 min, this process was repeated five times until the ideal thickness of the PCE was obtained. Finally, the phosphor coating was cured in an oven at a temperature of 150 °C for 1.5 h. Fig. 1 shows the cross-section of the PS PCE coating on the phosphor bearing surface of the stepped frustum. To have a better understand on this part, it's defined that the ith PS PCE is on the ith phosphor bearing surface along the z-axis direction. The α_i is defined as the angle between the tangent of the ith phosphor bearing surface and the x axis. The t_i is the thickness of the ith PS PCE, which is defined as the distance between the ith PS PCE surface and the ith phosphor bearing surface. The h_i represents the height of the ith PS PCE along the z-axis direction that is also the spraying direction.

It should be noticed that the α_i is determined by the fabrication of the stepped frustum. The t_i is measured six times to obtain the average results by the LEICA DM 2500 M microscope in order to reduce the measurement errors. The h_i is calculated through $t_i/\cos\alpha_i$. Table I shows the values of parameters α_i, t_i and h_i in detail. It can be seen that $h_{1,\text{average}} = 59.65$ μm, $h_{2,\text{average}} = 58.95$ μm and $h_{3,\text{average}} = 59.86$ μm, which clearly demonstrates that the h_i can be considered as a constant for different curvature of the phosphor bearing surface. It's mainly because that the phosphor mass per projection area along the spraying direction keeps constant. Consequently, it is convenient to predict the geometry of the PS PCE by the h_i and the geometry of the IL for remote pcLEDs.

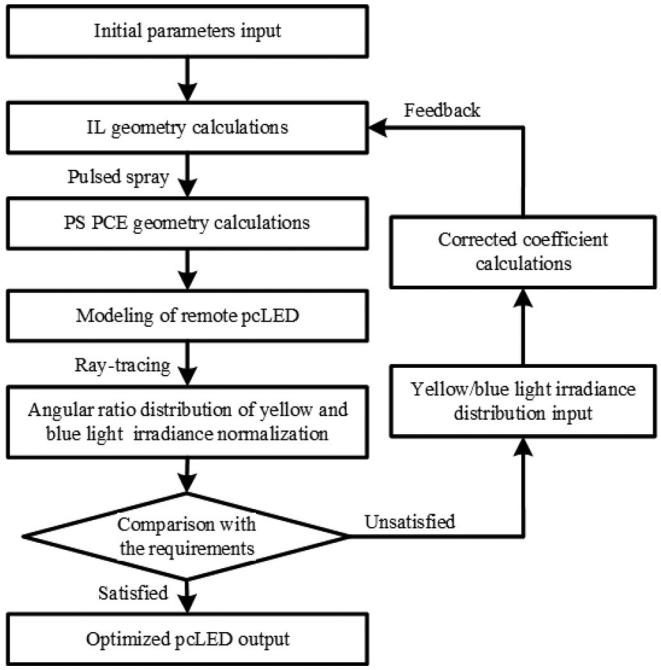

Fig. 2. PSFB method procedure for optimizing the ACU of remote pcLEDs.

III. METHODS

In order to effectively optimize the ACU of remote pcLEDs, we proposed the PSFB method combing the PS phosphor coating technique discussed above and the feedback iteration process. The PSFB method has two key points. One is that we use the curvature of the phosphor bearing surface to control the geometry of the PS PCE, which is based on the characteristic of the PS phosphor coating technique that the phosphor mass per projection area along the spraying direction is treated as constant (h_i keeps constant). The other is that we use the angular irradiance distributions of the yellow and blue light as feedback function to optimize the mass distribution of the PS PCE during the feedback iteration process. The process of the PSFB method is shown in Fig. 2, and the details of the illustrated steps are as follows: (1) Initial parameters input: the initial radius r of the IL, initial angular distribution of the correction coefficient $\text{Cor}_1(\theta_i)$, interval angle $\Delta\theta$, and terminal point a are input; (2) IL&PS PCE geometry calculations: the corrected geometry of the IL is calculated, and the geometry of the PS PCE sprayed on the IL surface is then determined; (3) Modeling of remote pcLED: the optical model of the pcLED is set up, and the normalized angular ratio distribution of the yellow and blue light irradiance $YB_{\text{nor},n}(\theta_i)$ is determined via the ray-tracing method; (4) Comparison with the requirements: if the standard deviation of $YB_{\text{nor},n}(\theta_i)$, $\sigma_{\text{YBnor},n}$, is no more than a, the current optimized pcLED is accepted; otherwise the step (5) should be conducted; (5) Feedback iteration: the yellow/blue light irradiance distribution is input to calculate the $\text{Cor}_n(\theta_i)$, and steps (2)–(4) must be repeated until $\sigma_{\text{YBnor},n} \leq a$.

To further explain this process, we present the calculations method in detail. Because pcLEDs are always approximately

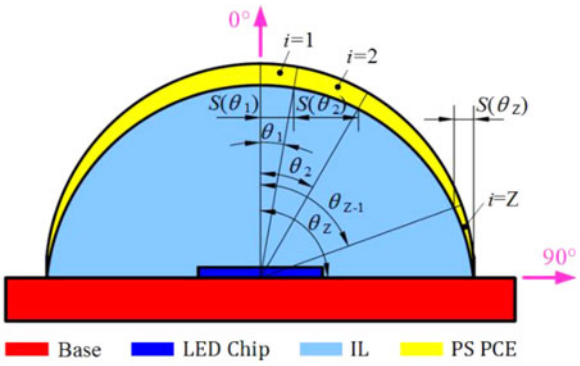

Fig. 3. Two-dimensional structure of remote pcLED based on PS phosphor-coating technology.

centrally symmetrical, we optimized the PS PCE in two dimensions for simplicity (considering the pcLED thickness to be sufficiently small), as shown in Fig. 3.

In this method, it is considered that the PS direction is parallel to the normal direction of the pcLED and that the mass of phosphor sprayed on the IL surface per projection area keeps constant. Therefore, the two-dimensional mass of the ith PS PCE unit $m(\theta_i)$ can be calculated as follows:

$$m\ (\theta_i) = s\,(\theta_i)\,k, \tag{1}$$

where

$$\theta_i = (i-1)\Delta\theta + \Delta\theta/2, \tag{2}$$

and k is the two-dimensional mass of phosphor sprayed per unit length (g/mm), $s(\theta_i)$ is the projected length of the ith PS PCE unit area along the PS direction (mm). As k is constant, the correction for $s(\theta_i)$ is equivalent to that for $m(\theta_i)$. Consequently, the two-dimensional coordinates of the IL surface $(x_n(\theta_i), y_n(\theta_i))$ and the PS PCE surface $(x'_n(\theta_i), y'_n(\theta_i))$ in the nth feedback iteration can be calculated based on the following forms:

$$x_n\ (\theta_i) = x'_n\ (\theta_{\mathrm{i}}) = \sum_{p=1}^{i} s_n(\theta_p), \tag{3}$$

$$y_n\ (\theta_i) = \begin{cases} x_n\ (\theta_i)/\tan\,(\theta_i)\,,\ i < Z \\ 0,\ i = Z \end{cases}, \tag{4}$$

and

$$y'_n\ (\theta_i) = y_n\ (\theta_i) + k/c = y_n\ (\theta_i) + h, \tag{5}$$

where

$$s_n\ (\theta_i) = s_0\ (\theta_i) \prod_{1}^{n} \mathrm{Cor}_n\,(\theta_i), \tag{6}$$

$$\mathrm{Cor}_n\ (\theta_i) = \begin{cases} \mathrm{Cor}_1\ (\theta_i)\,, n = 1 \\ Y B_0 f_n\ (\theta_i)/(I_{Y,n-1}\ (\theta_i)\,/I_{\mathrm{B},\ \mathrm{n-1}}\ (\theta_i))\,, n > 1 \end{cases}, \tag{7}$$

and $s_0(\theta_i)$ can be calculated based on the initial r of the IL input in step (1); Z is the total number of the PS PCE units from 0° to 90°; c is the two-dimensional mass per unit area of the PS PCE (g/mm^2); h is the height of the PS PCE along the PS direction (mm), which is a constant as shown in Section II; $I_{Y,n-1}(\theta_i)$ and $I_{B,n-1}(\theta_i)$, as feedback function, are the angular irradiance distributions of the yellow and blue light, respectively, in the $(n-1)$th feedback iteration (W/m^2); $\mathrm{Cor}_1(\theta_i)$ is the initial correction coefficient, which is generally equal to 1; $f_n(\theta_i)$ is the scale coefficient in the nth feedback iteration, which is used to ensure the stability of $\mathrm{Cor}_n(\theta_i)$; and YB_0 is the CCT reference coefficient, which is generally equal to $I_{Y,n-1}(0°)/I_{B,n-1}(0°)$. From equations (3) and (4), it can be known that the IL geometry in the nth feedback iteration is depended on the $s_n(\theta_i)$. And the $s_n(\theta_i)$ is modified by the $I_{Y,n-1}(\theta_i)$ and $I_{B,n-1}(\theta_i)$, which is shown in the equations (6) and (7). As a result, the IL geometry in the nth feedback iteration can be adjusted by the unbalanced $I_{Y,n-1}(\theta_i)$ and $I_{B,n-1}(\theta_i)$ directly. Moreover, with equations (3) and (5), the PS PCE geometry in the nth feedback iteration is also determined.

The pcLED modeling method mentioned in step (3) was proposed in our previous study [26]. In this step, the LED chip has dimensions of 1.16 mm × 1.16 mm × 0.1 mm, its refractive index is 2.43, and its emitted spectrum is centered at 455 nm. The IL with an initial $r = 1.3$ mm is made of silicon that is assumed not to absorb any light and has a refractive index of 1.54. The PS PCE is composed of YAG:Ce phosphor and silicon and has $h = 0.15$ mm, a mixed refractive index of 1.57, a conversion efficiency of 75%, an emitted spectrum centered at 565 nm, and a scattering coefficient of 43.10 mm^{-1}. The PS PCE is also assumed not to absorb any yellow light and to have an absorption coefficient of 11.62 mm^{-1} for blue light.

IV. Results and Discussion

Fig. 4 shows the IL geometries obtained by the PSFB method for N feedback iterations. When $N \leq 5$, the IL geometry changes significantly as N increases, and the maximum size change along the x direction between the nth and $(n-1)$th feedback iterations, $\Delta x_{\max}(n, n-1)$, is 1.67 mm. It's because that the $\mathrm{Cor}_n(\theta_i)$ changes obviously with increasing N as shown in the inset of Fig. 4(b), especially, the $\mathrm{Cor}_5(90°)$ is even three times less than the $\mathrm{Cor}_4(90°)$, resulting that the $x_5(90°)$ decreases significantly compared with the $x_4(90°)$ depended on equations (3), (6) and (7). Also, the IL geometry changes irregularly; the center and edges of the IL change either along the same direction (for example, between the second and third feedback iterations) or in opposite directions (for example, between the third and fourth feedback iterations). This irregularity is present because the CCT angular distribution is relatively nonuniform initially, causing $\mathrm{Cor}_n(\theta_i)$ to change significantly, as shown in the inset of Fig. 4(b). When $N > 5$, the IL geometry changes become smaller and more regular as N increases. Furthermore, the IL geometry exhibits no obvious changes after $N \geq 16$, $\Delta x_{\max}(n, n-1)$ decreases to 0.07 mm, and $\mathrm{Cor}_n(\theta_i)$ tends to 1. It's because that the IL geometry has been successful to modify the PS PCE geometry in order to balance the $I_Y(\theta_i)$ and $I_B(\theta_i)$, which also means that the $I_Y(\theta_i)/I_B(\theta_i)$ is almost the same among different viewing angles.

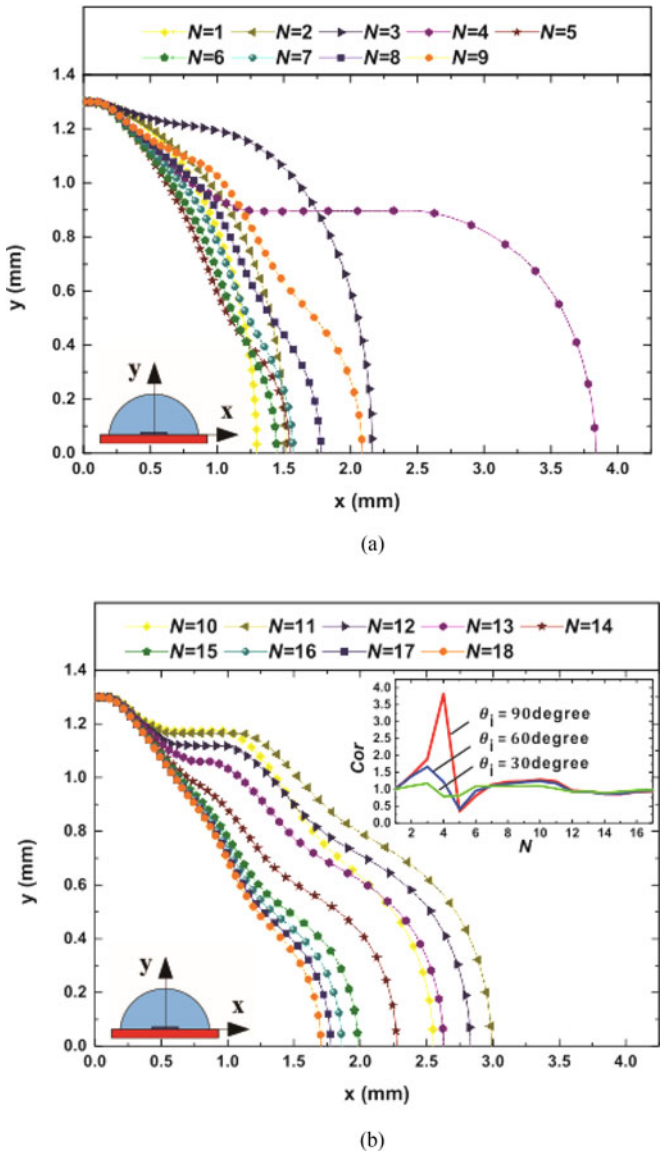

Fig. 4. IL geometry obtained by PSFB method in feedback iteration processes (a) $N = 1$ to $N = 9$ and (b) $N = 10$ to $N = 18$.

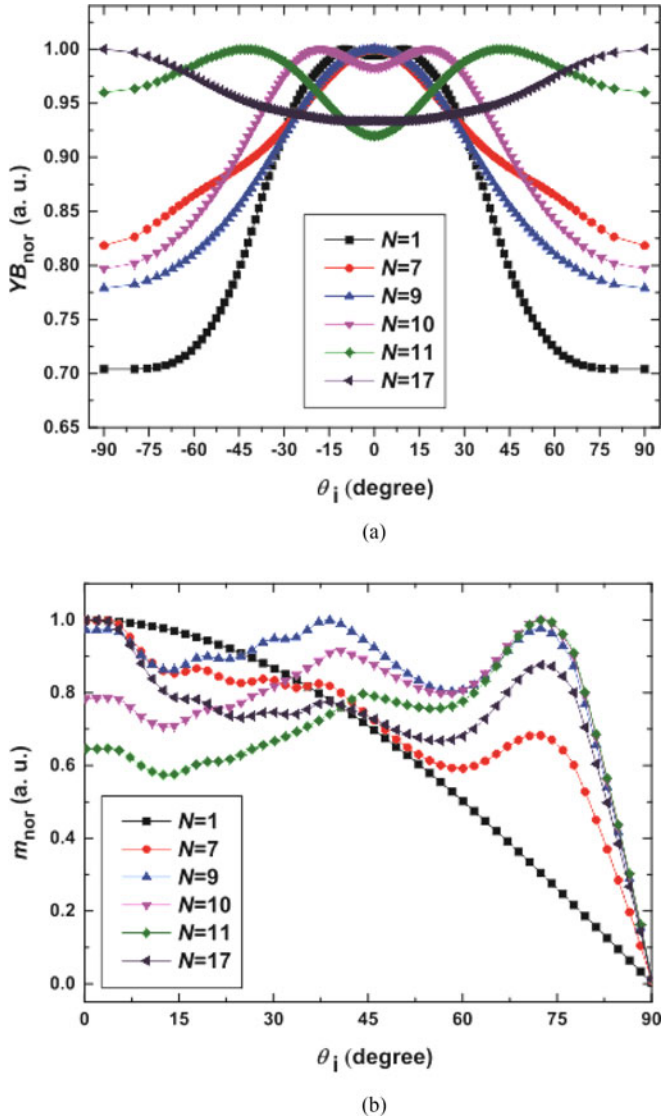

Fig. 5. (a) Distribution of normalized angular ratio of yellow to blue irradiance, $YB_{\mathrm{nor}}(\theta_i)$, and (b) normalized angular mass distribution of PS PCE, $m_{\mathrm{nor}}(\theta_i)$.

As the PSFB method mentioned above, the $YB_{\mathrm{nor}}(\theta_i)$ is used as feedback signals to adjust the geometry of PS PCE in order to optimize the ACU, and adjustments in the geometry of PS PCE are reflected in its mass distributions. To clarify the feedback effect on the ACU optimization, the normalized angular mass distribution of the PS PCE $m_{\mathrm{nor}}(\theta_i)$, and $YB_{\mathrm{nor}}(\theta_i)$ are shown in Fig. 5. Based on the feedback iteration results for $N = 1$, 7, 11, and 17 in Fig. 5(a), it is evident that the smaller (larger) part of $YB_{\mathrm{nor}}(\theta_i)$ increases (decreases) after several feedback iterations, causing $YB_{\mathrm{nor}}(\theta_i)$ to be more uniform throughout the entire feedback iteration process. For example, when $N = 7$, the central part of $YB_{\mathrm{nor},7}(\theta_i)$ is larger, but after several feedback iterations ($N = 11$), $YB_{\mathrm{nor},11}(\theta_i)$ $(-20^\circ < \theta_i < 20^\circ)$ becomes smaller than $YB_{\mathrm{nor},7}(\theta_i)$ $(-20^\circ < \theta_i < 20^\circ)$, while $YB_{\mathrm{nor},11}(\theta_i)$ $(20^\circ < \theta_i < 90^\circ)$ is larger than $YB_{\mathrm{nor},7}(\theta_i)$ $(20^\circ < \theta_i < 90^\circ)$. In the feedback iteration results for $N = 1$, 7, 11, and 17 in Fig. 5(b), it is interesting to note that the $m_{\mathrm{nor}}(\theta_i)$ changes with increasing N show almost the same tendency as those of $YB_{\mathrm{nor}}(\theta_i)$. For example, the center of $m_{\mathrm{nor},11}(\theta_i)$ decreases, while its edges increase compared with those of $m_{\mathrm{nor},7}(\theta_i)$. One plausible explanation is that $YB_{\mathrm{nor}}(\theta_i)$ mainly depends on the number of scattering and absorption events that have occurred in the PS PCE, which in turn mainly depends on the phosphor proportion. It also indicates that $m_{\mathrm{nor},n}(\theta_i)$ has a direct proportional relationship to $YB_{\mathrm{nor},n}(\theta_i)$ in the feedback iteration process.

Furthermore, the feedback iteration results for $N = 9$, 10, and 11 in Fig. 5 show that the center of $m_{\mathrm{nor},n}(\theta_i)$ decreases (increases) as N increases if the value of $YB_{\mathrm{nor},n-1}(\theta_i)$ is larger (smaller) at the center than at the edges. This behavior occurs because $m_{\mathrm{nor},n}(\theta_i)$ is inversely proportional to $YB_{\mathrm{nor},n-1}(\theta_i)$, which is evident based on equation (7). In conclusion, the inverse proportionality of $YB_{\mathrm{nor},n-1}(\theta_i)$ to $m_{\mathrm{nor},n}(\theta_i)$ and the direct proportional relationship between $YB_{\mathrm{nor},n}(\theta_i)$ and $m_{\mathrm{nor},n}(\theta_i)$

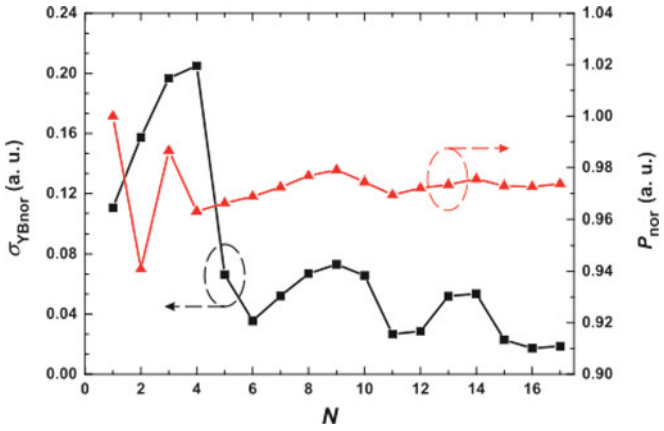

Fig. 6. Standard deviation of normalized angular ratio distribution of yellow and blue light irradiance σ_{YBnor} and normalized optical power P_{nor} of remote pcLED after different numbers of feedback iterations *N*.

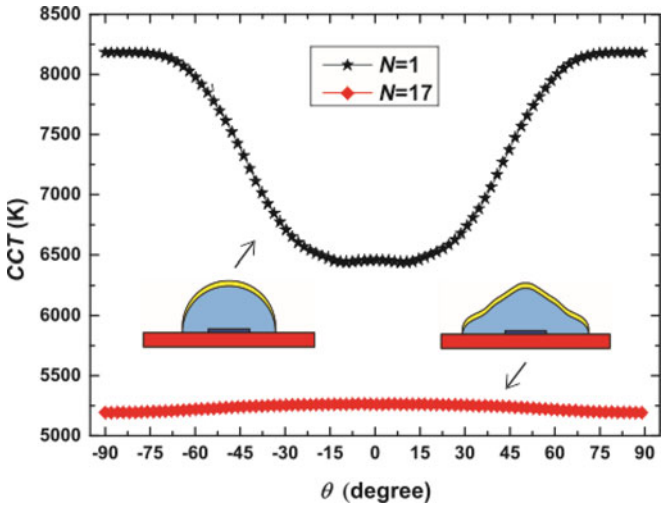

Fig. 7. CCT distributions of initial ($N = 1$) and final ($N = 17$) remote pcLEDs.

enable the feedback process through which the ACU of pcLEDs can be optimized.

To illustrate the direct effects of the PSFB method on the optical performance of the pcLED, σ_{YBnor} and the normalized optical power P_{nor} are shown in Fig. 6. It can be seen that σ_{YBnor} is 0.111 for the initial pcLED ($N = 1$) and generally decreases with increasing *N*. After $N \geq 14$, σ_{YBnor} shows only slight changes, and the final σ_{YBnor} value is 0.0186 ($N = 17$). Compared with the initial σ_{YBnor} value, the final σ_{YBnor} value is 83.2% lower, indicating that the ACU of the remote pcLED has been greatly improved because of the feedback effect mentioned above. On the other hand, P_{nor} has its highest value of 1 for the initial pcLED ($N = 1$), because the semi-spherical geometry of the IL facilitates the emission of LED light with a Lambert distribution. As N increases, P_{nor} also generally decreases; one reasonable explanation for this tendency is that the semi-spherical IL geometry is broken, causing the total inner reflection of the blue light to increase. After $N \geq 12$, P_{nor} also changes only slightly, and the final P_{nor} value is 0.974 ($N = 17$), which is only 2.6% lower than the initial P_{nor} value. Thus, the PSFB method effectively yields excellent ACU performance while decreasing the optical power only slightly.

Fig. 7 shows the final ($N = 17$) and initial ($N = 1$) CCT distributions of the remote pcLED, which are calculated by their angular power distribution of the blue and yellow light. The ACU of the initial pcLED is so poor that its CCT ranges from 6439 K to 8182 K with a maximum deviation of 1743 K, leading to the so-called "blue ring" phenomenon. This phenomenon results from the phosphor being uniformly sprayed on the semi-spherical IL surface; thus, there is relatively little phosphor at large viewing angles, causing fewer conversion events to occur and the blue light to be emitted from the pcLED more easily at large angles. After performing optimization by the method proposed in this study, the CCT of the final pcLED ranges from 5192 K to 5263 K with a maximum deviation of 71 K, 95.93% lower than that of the initial pcLED. As mentioned above, this decrease mainly results from $YB_{\mathrm{nor}}(\theta_i)$ being more uniform throughout the feedback iteration process due to the $m_{\mathrm{nor}}(\theta_i)$ correction. In addition, the CCT of the final pcLED is about 1500 K below the lowest CCT of the initial pcLED. One reasonable explanation for this change is that the projection area of the IL along the PS direction changes in the feedback iteration process (as shown in Fig. 4) and the *h* value of the PS PCE is kept constant, resulting that the total amount of the phosphor changes. Especially, the projection area of the final IL along the PS direction is larger than that of the initial IL. Therefore, the total amount of the phosphor of the final pcLED was greater than that of the initial pcLED, causing a higher probability of blue light conversion into yellow light in the final pcLED.

V. Conclusion

This study investigated the effect of the curvature of the phosphor bearing surface on the PCE geometry in PS phosphor coating process. Results show that the height of the PS PCE unit along the PS direction keeps constant though the curvature of the phosphor bearing surface is different. According to it, we further proposed a novel PSFB method that can effectively optimize the ACU of remote pcLEDs. The curvature of the IL surface was used to control the geometry of the PS PCE based on the characteristic of PS technique, and the yellow/blue light irradiance distribution was used as feedback function in order to optimize the mass distribution of PS PCE during the feedback iteration process. After 17 feedback iterations that used the feedback function to optimize the PS PCE, the CCT of the optimized remote pcLED ranged from 5192 K to 5263 K with a maximum deviation of 71 K, 95.93% lower than that of the initial remote pcLED, while P_{nor} only decreased by 2.6%. We considered that the ACU improvement mainly depends upon the inverse proportionality of $YB_{\mathrm{nor},n-1}(\theta_i)$ to $m_{\mathrm{nor},n}(\theta_i)$ and on the direct proportionality of $m_{\mathrm{nor}\,n}(\theta_i)$ to $YB_{\mathrm{nor},n}(\theta_i)$.

In future, we plan to further investigate this method to design the CCT distribution and apply it to different LED packaging structures, we believe that our finding will significantly contribute to the development of LED lighting applications.

REFERENCES

[1] P. Pust, P. J. Schmidt, and W. Schnick, "A revolution in lighting," *Nature Mater.*, vol. 14, pp. 454–458, 2015.

[2] C.-Y. Liu *et al.*, "Improvement of emission uniformity by using micro-cone patterned PDMS film," *Opt. Express*, vol. 22, pp. 4516–4522, 2014.

[3] H.-Y. Lin *et al.*, "Improvement of light quality by DBR structure in white LED," *Opt. Express*, vol. 23, pp. A27–A33, 2015.

[4] X. Ding *et al.*, "Improving LED CCT uniformity using micropatterned films optimized by combining ray tracing and FDTD methods," *Opt. Express*, vol. 23, pp. A180–A191, 2015.

[5] H. Xiao *et al.*, "Improvements on optical and chromatic uniformities of light-emitting diodes with microscale-roughness-controlled surfaces," *IEEE Photon. Technol. Lett.*, vol. 7, pp. 1–8, 2015.

[6] H. Zheng, S. Liu, and X. Luo, "Enhancing angular color uniformity of phosphor-converted white light-emitting diodes by phosphor dip-transfer coating," *J. Lightw. Technol.*, vol. 31, no. 12, pp. 1987–1993, Jun. 2013.

[7] H. Zheng *et al*., "Dip-transfer phosphor coating on designed substrate structure for high angular color uniformity of white light emitting diodes with conventional chips," *Opt. Express*, vol. 21, pp. A933–A941, 2013.

[8] Z.-Y. Liu, C. Li, B.-H. Yu, Y.-H. Wang, and H.-B. Niu, "Uniform white emission of WLEDs realized by multilayer phosphor with pyramidal shape and inversed concentration distribution," *IEEE Photon. Technol. Lett.*, vol. 24, no. 17, pp. 1558–1560, Sep. 2012.

[9] H.-T. Huang, C.-C. Tsai, and Y.-P. Huang, "Conformal phosphor coating using pulsed spray to reduce color deviation of white LEDs," *Opt. Express*, vol. 18, pp. A201–A206, 2010.

[10] H. Zheng *et al.*, "Conformal phosphor coating using capillary microchannel for controlling color deviation of phosphor-converted white light-emitting diodes," *Opt. Express*, vol. 20, pp. 5092–5098, 2012.

[11] H. Zheng, J. Ma, and X. Luo, "Conformal phosphor distribution for white lighting emitting diode packaging by conventional dispensing coating method with structure control," *IEEE Trans. Compon. Packag. Technol.*, vol. 3, no. 3, pp. 417–421, Mar. 2013.

[12] C.-H. Chiang *et al.*, "Effects of phosphor distribution and step-index remote configuration on the performance of white light-emitting diodes," *Opt. Express*, vol. 40, pp. 2830–2833, 2015.

[13] H. Luo *et al.*, "Analysis of high-power packages for phosphor-based white-light-emitting diodes," *Appl. Phys. Lett.*, vol. 86, 2005, Art. no. 243505.

[14] H. Zheng, X. Fu, R. Hu, S. Liu, and X. Luo, "Angular color uniformity improvement for phosphor-converted white light-emitting diodes by optimizing remote coating phosphor geometry," in *Proc. 13th Int. Conf. Electron. Packag. Technol. High Density Packag.*, 2012, pp. 1483–1486.

[15] Y.-H. Won *et al.*, "Effect of phosphor geometry on the luminous efficiency of high-power white light-emitting diodes with excellent color rendering property," *Opt. Lett.*, vol. 34, pp. 1–3, 2009.

[16] R. Yu, S. Jin, S. Cen, and P. Liang, "Effect of the phosphor geometry on the luminous flux of phosphor-converted light-emitting diodes," *IEEE Photon. Technol. Lett.*, vol. 22, no. 23, pp. 1765–1767, Dec. 2010.

[17] Z. Liu, S. Liu, K. Wang, and X. Luo, "Optical analysis of color distribution in white LEDs with various packaging methods," *IEEE Photon. Technol. Lett.*, vol. 20, no. 24, pp. 2027–2029, Dec. 2008.

[18] S.-P. Ying, H.-K. Fu, and H.-Z. Tu, "Curved remote phosphor structure for phosphor-converted white LEDs," *Appl. Opt.*, vol. 53, pp. H160–H164, 2014.

[19] S. Wang, X. Chen, M. Chen, H. Zheng, H. Yang, and S. Liu, "Improvement in angular color uniformity of white light-emitting diodes using screen-printed multilayer phosphor-in-glass," *Appl. Opt.*, vol. 53, pp. 8492–8498, 2014.

[20] M.-T. Wang and J.-M. Huang, "Accurate control of chromaticity and spectra by feedback phosphor-coating," *Opt. Express*, vol. 23, pp. 11576–11585, 2015.

[21] H.-C. Kuo *et al.*, "Patterned structure of remote phosphor for phosphor-converted white LEDs," *Opt. Express*, vol. 19, pp. A930–A936, 2011.

[22] H.-T. Lin, C.-H. Tien, C.-P. Hsu, and R.-H. Horng, "White thin-film flip-chip LEDs with uniform color temperature using laser lift-off and conformal phosphor coating technologies," *Opt. Express*, vol. 22, pp. 31646–31653, 2014.

[23] B.-C. Lin *et al.*, "Luminous efficiency enhancement of white light-emitting diodes by using a hybrid phosphor structure," *J. Photon. Energy*, vol. 5, 2015, Art. no. 057603.

[24] Cree, "Technical Datasheet XLamp® XT-E LEDs." (2012). [Online]. Available: http://www.cree.com/xlamp

[25] Z.-T. Li, Y. Tang, Z.-Y. Liu, Y.-E. Tan, and B.-M. Zhu, "Detailed study on pulse-sprayed conformal phosphor configurations for LEDs," *J. Display Technol.*, vol. 9, pp. 433–440, 2013.

[26] J. Li *et al.*, "A detailed study on phosphor-converted light-emitting diodes with multi-phosphor configuration using the finite-difference time-domain and ray-tracing methods," *IEEE J. Quantum Electron.*, vol. 51, no. 10, pp. 1–10, Oct. 2015.

Jia-Sheng Li received the B.E. degree in mechanical engineering and automation from South China University of Technology, Guangzhou, China, in 2014. He has been working toward the Postgraduate degree at the Key Laboratory of Surface Functional Structure Manufacturing of Guangdong High Education Institutes, South China University of Technology, Guangdong, China.

His current research interests include packaging process, optical simulation, and lighting quality of LED.

Yong-Hui Chen received the B.E. degree in mechanical engineering and automation from South China University of Technology, Guangzhou, China, in 2014. He has been working toward the Postgraduate degree at the Key Laboratory of Surface Functional Structure Manufacturing of Guangdong High Education Institutes, South China University of Technology, Guangdong, China.

His current research interest includes flue cell and its applications in LED.

Zong-Tao Li received the Ph.D. degree in microelectronics manufacture engineering in mechanical engineering from South China University of Technology, Guangzhou, China, in 2014.

He is also with the Key Laboratory of Surface Functional Structure Manufacturing of Guangdong High Education Institutes, South China University of Technology, Guangdong, China, and with the Optoelectronics Engineering Technology Research and Development Center, Foshan Nationstar Optoelectronics Co. Ltd., Foshan, China. His major research interests include packaging of high-power LEDs, lighting quality, and device reliability.

Shu-Dong Yu received the B.E. degree in mechanical engineering and automation from South China University of Technology, Guangzhou, China, in 2014. He has been working toward the Postgraduate degree at the Key Laboratory of Surface Functional Structure Manufacturing of Guangdong High Education Institutes, South China University of Technology, Guangdong, China.

His current research interests include LED packaging and lighting quality.

Yong Tang received the Ph.D. degree in mechanical engineering from South China University of Technology, Guangzhou, China, in 1994.

He has more than 10 years of experience in surface coating technology and more than 8 years in optoelectronic LED packaging. He is currently a Professor with the School of Mechanical and Automotive Engineering, South China University of Technology, and the Director of the Key Laboratory of Surface Functional Structure Manufacturing of Guangdong High Education Institutes, Guangdong, China. His research interests include surface properties in clean energy and its high efficient usage, especially in energy-saving solid-state lighting.

Xin-Rui-Ding received the Ph.D. degree in microelectronics manufacture engineering in mechanical engineering from South China University of Technology, Guangzhou, China, in 2015.

He is with the Key Laboratory of Surface Functional Structure Manufacturing of Guangdong High Education Institutes, South China University of Technology, Guangdong, China. His major research interests include the LED packaging, lighting quality, and reliability.

Wei Yuan received the Ph.D. degree in microelectronics manufacture engineering in mechanical engineering from the South China University of Technology, Guangzhou, China, in 2012.

He is with the Key Laboratory of Surface Functional Structure Manufacturing of Guangdong High Education Institutes, South China University of Technology, Guangdong, China. His major research interests include the fuel cell and its applications in LED.